Springer

KSME

Journal of Mechanical Science and Technology 25 (8) (2011) 1893~1904
www.springerlink.com/content/1738-494x
DOI 10.1007/s12206-011-0517-6

A statistical characterization method for damping material properties and its application to structural-acoustic system design †

Byung C. Jung[1], Dooho Lee[2,*], Byeng D. Youn[3,**] and Soobum Lee[4]

[1]*Department of Mechanical Engineering, University of Maryland, College Park, MD, 20742, USA*
[2]*Department of Mechanical Engineering, Dongeui University, Busan, 614-714, Korea*
[3]*School of Mechanical and Aerospace Engineering, Seoul National University, Seoul, 151-742, Korea*
[4]*Department of Aerospace and Mechanical Engineering, University of Notre Dame, Notre Dame, IN, 46556, USA*

(Manuscript Received November 30, 2010; Revised March 16, 2011; Accepted April 22, 2011)

Abstract

The performance of surface damping treatments may vary once the surface is exposed to a wide range of temperatures, because the performance of viscoelastic damping material is highly dependent on operational temperature. In addition, experimental data for dynamic responses of viscoelastic material are inherently random, which makes it difficult to design a robust damping layout. In this paper a statistical modeling procedure with a statistical calibration method is suggested for the variability characterization of viscoelastic damping material in constrained-layer damping structures. First, the viscoelastic material property is decomposed into two sources: (i) a random complex modulus due to operational temperature variability, and (ii) experimental/model errors in the complex modulus. Next, the variability in the damping material property is obtained using the statistical calibration method by solving an unconstrained optimization problem with a likelihood function metric. Two case studies are considered to show the influence of the material variability on the acoustic performances in the structural-acoustic systems. It is shown that the variability of the damping material is propagated to that of the acoustic performances in the systems. Finally, robust and reliable damping layout designs of the two case studies are obtained through the reliability-based design optimization (RBDO) amidst severe variability in operational temperature and the damping material.

Keywords: Constrained-layer damping layout; Statistical modeling of viscoelastic material; Statistical calibration method; Structural-acoustic system; Reliability-based design optimization

1. Introduction

Many researchers in noise and vibration areas have focused on developing an effective method of noise suppression against vibrating structures using viscoelastic material. Examples include damping sheets on the body structure of passenger cars, airplanes, ships, and ducts in buildings and electric appliances. The importance of the optimal damping layout design has been emphasized for low-cost, high-efficiency damping. However, it is difficult to acquire a robust damping layout design because viscoelastic materials possess frequency- and temperature-dependent dynamic properties. In most cases surface damping layers are exposed to open air and hence are operated under a wide range of temperatures that varies periodically and randomly. As a result, substantial variations in the damping material properties have been observed in the service life of the materials; these variations cause the degradation of damping performance for noise/vibration reduction. In addition, the inherent errors in experimental data (e.g., experimental noise and measurement errors) caused by the difficulty in measuring the dynamic responses of viscoelastic material make it difficult to design a robust damping layout. Even though a fractional derivative model [1] is often used to describe frequency- and temperature-dependent dynamic characteristics of damping material, this model still contains a model error (or uncertainty).

Many researchers have suggested various kinds of optimal design formulations on damping layout structures [2-9]. In these investigations, damping performances were maximized by controlling structural dimensions and/or damping properties. However, these works do not consider the variability of damping materials. Recently, the authors' study suggested an approach to characterize the variability in the damping material properties and applied the approach to a constrained-layer damping layout design to maximize structural damping performance [10]. In the material characterization method used in this previous work, the variability in the damping material was

† This paper was recommended for publication in revised form by Editor Yeon June Kang

* Corresponding author. Tel.: +82 51 890 1658, Fax.: +82 51 890 2232
** Co-corresponding author. Tel.: +82 2 880 1919, Fax.: +82 2 880 8302
E-mail address: dooho@deu.ac.kr, bdyoun@snu.ac.kr

extracted from the unbiased estimator of the variance and the confidence interval (CI) of the master curve at a reference temperature. However, the method has limitations in that it is only applicable to the fractional derivative model and the information available in experimental data was not fully utilized. It is because the method utilized the relationship between storage shear modulus data and parameters in the fractional derivative model to characterize the material variability.

Our aim was to design a robust constrained-layer damping layout to maximize the acoustic damping efficiency while considering the variability of damping material properties due to operational temperature, experimental error and model error in structural-acoustic system. For this purpose, a statistical calibration method is proposed for the variability characterization of unknown input model parameters through comparison of the predicted and observed outputs [11]. The statistical calibration method can be generally used for any viscoelastic constitutive models such as a fractional derivative model, a Golla-Hughes-McTavish model [12], etc. Current statistical model calibration is mainly based on methods of moments [13], Bayesian statistics [14-18] and maximum likelihood estimation [19]. In this study an optimization technique is integrated with the eigenvector dimension reduction (EDR) method to maximize the likelihood function to determine the parameters of the unknown variability. This paper is organized as follows: In Section 2, a hybrid model for a structural-acoustic system analysis and the EDR method [20] for effective probability analyses are briefly explained. Section 3 presents a variability characterization approach of a viscoelastic damping layer and the approach is applied to a damping material. In Section 4, reliability-based design optimization (RBDO) is carried out to determine an optimal robust design of two different constrained-layer damping layouts in structural-acoustic systems.

2. Statistical approach for structural-acoustic system analysis

For the statistical structural-acoustic system analysis, this work combines three techniques: 1) a boundary-element analysis, 2) a viscoelastic constitutive model, and 3) the eigenvector dimension reduction (EDR) method. A boundary-element analysis is employed to calculate an acoustic response of a structural-acoustic system. As a viscoelastic constitutive model, the fractional derivative model is chosen to demonstrate variability characterization of the damping material property. The EDR method is used for the uncertainty propagation and reliability analyses to calculate reliability for the RBDO.

2.1 Boundary-element analysis of structural-acoustic systems

To compute an acoustic response of a structural-acoustic system, it is assumed that the structural-acoustic system is semicoupled, that is, the structural responses influence the acoustic responses but the acoustic responses do not affect the vibration of the structures. As a result, structural-acoustic problems can be solved sequentially. Finite element analysis for structural response and boundary element analysis for acoustic response are used in this study. The detailed procedures for these analyses can be found in Ref. [4]. The air density and the speed of sound are given as functions of temperature:

$$\rho = p_0 / (R \cdot T),\ c = 331.3 \cdot \sqrt{1 + T/(273.15)} \tag{1}$$

where ρ is the air density, c is the speed of sound, p_0 is sea-level standard atmospheric pressure, R is the specific gas constant, and T is temperature in Kelvin.

The constrained-layer damping beam in this work consists of three layers: a base beam, a viscoelastic damping layer, and a constraining layer. To compute structural responses of the constrained-layer damping beam, a 10-DOF finite element is used. The eigenvalue problem of the constrained-layer damping beam problem is defined as:

$$\mathbf{Ky} = \lambda c\mathbf{My}. \tag{2}$$

Here, **M** and **K** represent the global mass and stiffness matrices, respectively, and **y** is the complex eigenvector and λ^c is the complex eigenvalue. The stiffness matrix **K** becomes a complex-valued and frequency-dependent matrix due to the viscoelastic damping layer. The natural frequency ψ_k and the modal loss factor η_k of the k-th mode are defined as:

$$\psi_k = \frac{\sqrt{\mathrm{Re}(\lambda_k^c)}}{2\pi},\quad \eta_k = \frac{\mathrm{Im}(\lambda_k^c)}{\mathrm{Re}(\lambda_k^c)} \tag{3}$$

where Re(•) and Im(•) refer the real and the imaginary parts of the argument, respectively. To calculate the forced responses of the constrained-layer damping beam, the modal superposition method is used.

2.2 Fractional derivative model

The fractional derivative model is one of the most popular models in describing frequency-dependent characteristics of viscoelastic damping materials because of accuracy and simplicity of the model. In the fractional derivative model of order one, the constitutive equation is given as follows:

$$\sigma(t) + c_1 D^\beta \sigma(t) = a_0 \varepsilon(t) + a_1 D^\beta \varepsilon(t) \tag{4}$$

where $0 < \beta < 1$, and D^β indicates the fractional derivative [1]. a_0, a_1, c_1, and β are the four variables of fractional derivative model. The Fourier transform gives a complex modulus expression as

$$\tilde{\sigma} = E^* \tilde{\varepsilon} = (E' + \mathrm{i}E'')\tilde{\varepsilon} = \frac{a_0 + a_1[\mathrm{i}f]^\beta}{1 + c_1[\mathrm{i}f]^\beta}\tilde{\varepsilon} \tag{5}$$

where ~ refers to the Fourier transform and f is frequency. E' and E'' are storage and loss moduli, respectively. Introducing the shift factor from the temperature-frequency equivalence hypothesis, the temperature-dependent characteristics of the complex modulus can be described as follows:

$$E^* = (E' + \mathrm{i}E'') = \frac{a_0 + a_1[\mathrm{i}f\alpha(T)]^\beta}{1 + c_1[\mathrm{i}f\alpha(T)]^\beta} \tag{6}$$

where $\alpha(T)$ is the shift factor and $f\alpha$ is called as reduced frequency. Knowing the shift factor at any given temperature (T) and a master curve at a reference temperature T_0, the complex modulus can be predicted from Eq. (6). The shift factor and temperature can be related by the Arrhenius equation as

$$\log[\alpha(T)] = d_1(1/T - 1/T_0) \tag{7}$$

where d_1 is a material constant. It is known that the four-variable fractional derivative model sufficiently represents the real behavior of viscoelastic material over a wide frequency range [21]. Finally, it is evident that the complex modulus expression of Eq. (6) can be applied to the shear modulus as well as Young's modulus. Therefore, in this paper the complex Young's modulus and complex shear modulus will not be distinguished in symbols hereafter.

2.3 Eigenvector dimension reduction (EDR) method

Uncertainty propagation and reliability analysis are necessary to characterize the variability of the viscoelastic damping layer in Section 3 and to calculate reliability for RBDO in Section 4. Among uncertainty propagation analysis methods, the eigenvector dimension reduction (EDR) method [20] has been chosen here because it requires only three or five samples (responses of the structural-acoustic systems) for one random variable along the eigenvectors of random input variables. The EDR method approximates the statistical moments (e.g., mean, standard deviation, skewness, kurtosis) of a system response and its probability density function (PDF). In general, the statistical moments of the system response, $Y(\mathbf{X})$, can be calculated as

$$E\left\{Y^m(\mathbf{X})\right\} = \int_{-\infty}^{\infty}\int_{-\infty}^{\infty} Y^m(\mathbf{x}) \cdot f_{\mathbf{X}}(\mathbf{x}) \cdot d\mathbf{x},\ m = 0,1,2,\cdots \tag{8}$$

where Y is the system response, $E\{\bullet\}$ indicates the expectation operator, and $f_{\mathrm{X}}(\mathbf{x})$ is the joint probability density function (PDF) of $\mathbf{X}$. Multi-dimensional integration in Eq. (8) can be converted into multiple one-dimensional integrations using an additive decomposition (Y_{a}) [22], defined as

$$\begin{aligned} &Y(X_1,...,X_N) \cong Y_a(X_1,...,X_N) = \\ &\sum_{j=1}^{N} Y(\mu_1,...,\mu_{j-1},X_j,\mu_{j+1},...,\mu_N) - (N-1)Y(\mu_1,...,\mu_N) \end{aligned} \tag{9}$$

where N is the number of random variables and μ indicates the mean of random variables. Although the additive decomposition (Y_{a}) ignores all the interactive terms, the error produced is less than that of a second-order Taylor expansion method for probability analysis [20]. With the help of the additive decomposition, the m^{th} statistical moments for the response can be approximately obtained as

$$\begin{aligned} &E\left[Y_a^m(\mathrm{X})\right] = \\ &E\left\{\left[\sum_{j=1}^{N} Y\left(\mu_1,\cdots,X_j,\cdots,\mu_N\right) - (N-1)\cdot Y\left(\mu_1,\cdots,\mu_N\right)\right]^m\right\}. \end{aligned} \tag{10}$$

Using a binomial formula, Eq. (10) can be evaluated by executing one-dimensional integration recursively. To solve the one-dimensional integration effectively, the EDR method incorporates three technical components: 1) the eigenvector sampling method to handle correlated and asymmetric random input variables, 2) the stepwise moving least-squares method for one-dimensional response approximation, and 3) a stabilized Pearson system for generating a PDF of a response. It is shown that the EDR method is sufficiently accurate to calculate the PDF and reliability in structural-acoustic systems in Section 4.

3. Statistical characterization of the viscoelastic damping material property

The damping performance of a constrained-layer damping structure is related to the dynamic properties of the viscoelastic damping material. However, the dynamic properties of the damping material are highly sensitive to the environmental temperature and/or chemical composition of the material. In this section we propose a statistical approach to characterize the variability of the viscoelastic damping material, and show the consequence of variability in the damping material on the variability of the dynamic response of the structural-acoustic systems.

3.1 Variability decomposition of the viscoelastic damping material

The variability in the dynamic material properties of viscoelastic material primarily results from two sources: 1) operational temperature variation and 2) experimental/model errors associated with the viscoelastic damping material. To characterize the variability in the viscoelastic damping material properties, the complex modulus of the damping material can be expressed as [4] follows:

$$\begin{aligned} E^*(f,T) &= E_1^*(T) + \varepsilon_E^*(f,T_0) \\ E_1^*(T) &= \frac{\mu_{a_0} + \mu_{a_1}[\mathrm{i}f\alpha(T)]^{\mu_\beta}}{1 + \mu_{c_1}[\mathrm{i}f\alpha(T)]^{\mu_\beta}} \end{aligned} \tag{11}$$

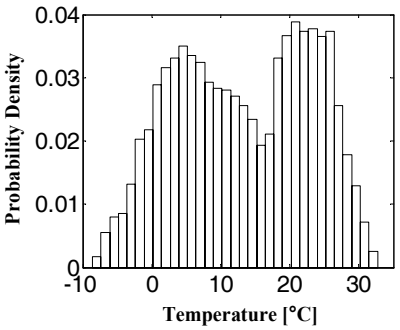

Fig. 1. Temperature histogram of Seoul in 2007.

$$\varepsilon_E^*(f,T_0)=\frac{a_0+a_1[if\alpha(T_0)]^\beta}{1+c_1[if\alpha(T_0)]^\beta}-\frac{\mu_{a_0}+\mu_{a_1}[if\alpha(T_0)]^{\mu_\beta}}{1+\mu_{c_1}[if\alpha(T_0)]^{\mu_\beta}}.$$

$E^*(f,T)$ indicates the uncertain complex modulus of the viscoelastic damping material, which is decomposed into two terms: the random complex modulus (E_1^*) and the error in the complex modulus (ε_E^*). E_1^* considers the operational temperature variability, whereas ε_E^* considers experimental/model errors at a given temperature (T_0). It is assumed that $\varepsilon_E^*(f)$ is the function of frequency only and follows a Gaussian process. We need to determine the statistical information of two terms ($E_1^*(f,T)$ and $\varepsilon_E^*(f)$) to characterize the variability in $E^*(f,T)$. The variability of E_1^* and ε_E^* is characterized using the Arrhenius equation, the fractional derivative model and statistical calibration method in the next section.

3.2 Variability characterization using a statistical calibration method

For the characterization of the random complex modulus, $E_1^*(f,T)$, an environmental temperature variation was first characterized with hourly temperature data measured for one year in Seoul as shown in Fig. 1.

The variation in the temperature profile in Fig. 1 results in the variation in the Arrhenius shift factor (α) in Eq. (7). Sequentially, the variation in the Arrhenius shift factor propagates to the one in the complex modulus. It is thus definite that the storage shear modulus and the loss factor vary significantly due to the temperature variation, and the variation of the material properties can also affect the dynamic responses of structural-acoustic systems.

For the error in the complex modulus, ε_E^*, the statistical calibration method is employed to characterize the variability. The statistical calibration determines the unknown variability parameter vector ($\boldsymbol{\theta}$) of the four fractional derivative model variables (a_0, a_1, c_1, and β) while maximizing the agreement between the predictive response of the fractional derivative model and experimental data (storage shear modulus and loss factor data). The variability of the model variables (a_0, a_1, c_1, and β) can be represented by statistical parameters of a suitable distribution. For example, in case of the normal distribution, the $\boldsymbol{\theta}$ includes means and standard deviations of the model variables. The statistical calibration is defined as the optimization problem as follows:

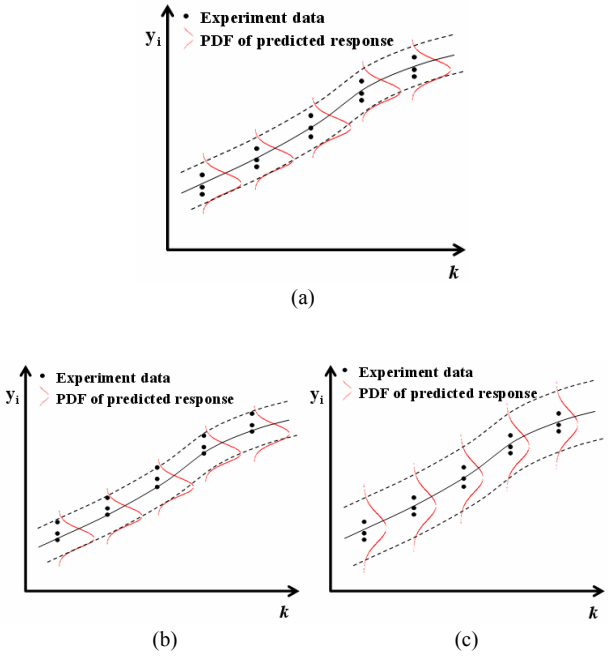

Fig. 2. The concept of the likelihood function in the statistical calibration method: (a) High likelihood function; (b) Low likelihood function due to deviated mean values; (c) Low likelihood function due to large standard deviations.

$$\text{maximize} \quad L(\boldsymbol{\theta}\,|\,\mathbf{y})=\sum_{i=1}^{q}\log_{10}[p(y_i\,|\,\boldsymbol{\theta})] \tag{12}$$

where y_i is a component of the random response vector $\mathbf{y}$ (e.g., experimental data), L is the likelihood function, q is the number of experimental data, and p is a PDF of y for a given $\boldsymbol{\theta}$. The likelihood function is used as a metric to measure the goodness of agreement between the response PDF and experimental data. After the generation of response PDF (p in Eq. (12)) using the EDR method, the probability density of the particular experimental data is calculated. The optimal $\boldsymbol{\theta}$ can be obtained by maximizing the likelihood function. A gradient-based optimizer in MATLAB [23] is used to solve the unconstrained optimization problem in Eq. (12). Fig. 2 shows the concept of the likelihood function in the statistical calibration method. In the figure, k indicates a controllable variable (e.g., reduced frequency in the complex modulus), and y denotes experimental data or predicted responses (e.g., storage shear modulus or loss factor in the complex modulus).

The likelihood function between the experimental data and the response PDFs of Fig. 2(a) is larger than those of Figs. 2(b) or (c): this is because the mean values of the response PDFs in Fig. 2(b) are deviated from those of experimental data, and the standard deviations of the PDF in Fig. 2(c) are larger than those of Fig. 2(a). Fig. 3 summarizes the procedure of the

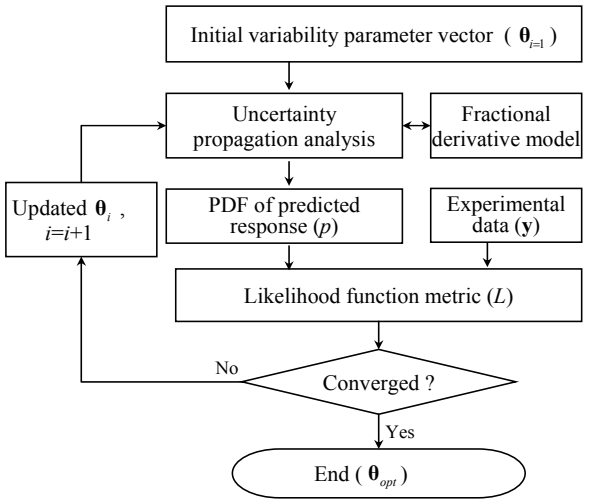

Fig. 3. The procedure of the statistical calibration method.

statistical calibration method. By combining the likelihood function metric and optimization technique, this statistical calibration method can determine the most suitable variability information of the complex modulus parameters for the best description of the experimental data (storage shear modulus and loss factor data).

3.2.1 Case study: variability characterization of the ISD-110 damping material

In this section, the variability characterization method is applied to a damping material, 3M ISD-110, which is a typical damping adhesive generally used in constrained-layer damping. Using the sandwich beam test data (storage shear modulus and loss factor data) in Ref. [1], the master curve at a reference temperature (T_0) and the variables of the fractional derivative model are estimated. Fig. 4 shows the uncertainty propagation map for variability characterization. Each side of the diagram in Fig. 4 displays the variability propagation for $E_1^*(f,T)$ and ε_E^*, respectively. First, for the characterization of $E_1^*(f,T)$, the uncertainty propagation using Monte Carlo simulation is employed using the temperature profile results in Fig. 1, Eqs. (5) and (7). The effect of the material constant (d_1) on the shift factor (α) is ignored during the Monte Carlo simulation, even though α is a function of both T (operational temperature) and d_1, due to its negligible effect on α. The estimated statistics of temperature and log(α) are listed in Table 1.

Next, for the variability of ε_E^*, the statistical calibration method is applied with the experimental data of ISD-110. Fig. 5 shows the log-log plots of the experimental data (dots) at a reference temperature T_0 and the master curve (the solid line) of the complex modulus. The statistical properties of the model variables in the master curve are listed in Table 1.

To define the variability parameter vector in Eq. (12) for the statistical calibration method, it is first assumed that logarithmic values of the three fractional derivative model variables (log(a_0), log(a_1), log(c_1)) and β follow normal distribution.

Table 1. Properties of random variables for ISD-110 damping material ($\gamma_{\log(a1),\log(c1)}$=0.4239).

Random variable	Mean	Standard deviation	Distribution type
Temperature(℃)	13.28	9.79	Bimodal data
log(α)	-1.14	0.63	Bimodal
log(a_0)	log(0.0287)	0.06897	Normal
log(a_1)	log(1.0350)	0.05360	Normal
log(c_1)	log(0.0115)	0.05360	Normal
β	0.5	0.05574	Normal

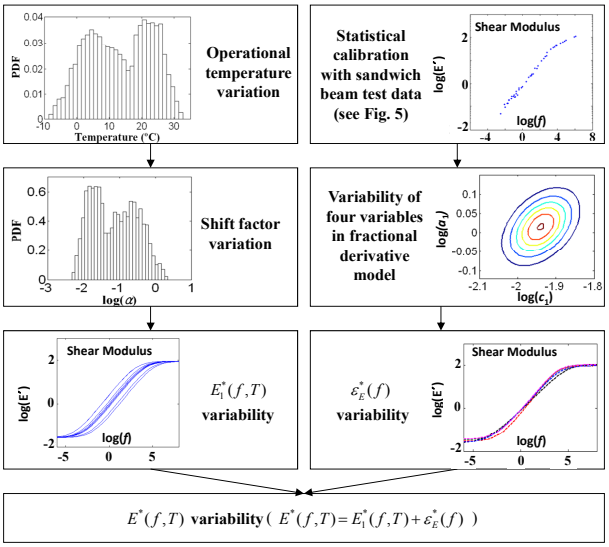

Fig. 4. Uncertainty propagation map for variability characterization.

Because log(a_1/c_1) is equal to the asymptotic logarithmic value of the storage shear modulus, in the high frequency range (around 10^8 Hz in Fig. 5), log(a_1) is linearly proportional to log(c_1), say, log(a_1/c_1) = constant or log(a_1) = log(c_1) + constant. Therefore, the principal directions of the anticipated joint PDF are [-1, 1] and [1, 1], which means that log(a_0) and log(c_1) have identical standard deviations and correlation coefficients [10]. Then, the variability parameter vector, $\boldsymbol{\theta}$, is decided as $\{s_{\log(a0)}, s_\beta, s_{\log(a1),\log(c1)}, \gamma_{\log(a1),\log(c1)}\}$, where s and γ indicate standard deviation and correlation coefficient, respectively. The experimental data shown in Fig. 5(a) and (b) are employed to calculate the likelihood function. Optimal values of the parameter vector, $\boldsymbol{\theta}$, are obtained by solving the optimization problem in Eq. (12). The calibrated statistics of four parameters are listed in Table 1. When compared to Ref. [10], the standard deviation of β is significantly increased due to the consideration of the loss factor data in the variability characterization process. The increased standard deviation results in the wider 95% confidence interval (see Fig. 5) for the storage shear modulus and the loss factor than those in Ref. [10]. The characterized material parameters in Table 1 are used for RBDO of the constrained-layer damping layout in Section 4.

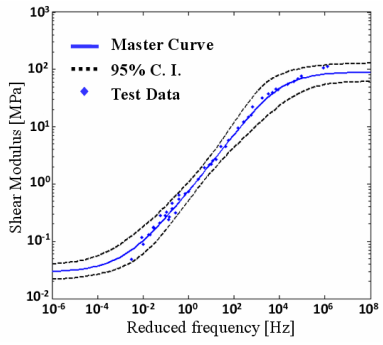

(a)

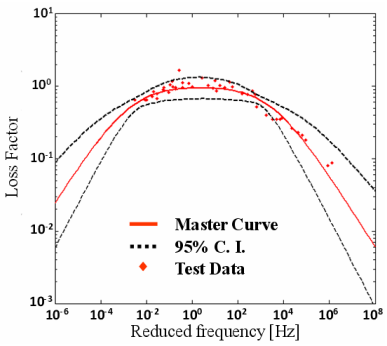

(b)

Fig. 5. Experimental data, master curve, 95% CI of ISD-110: (a) Storage shear modulus; (b) Loss factor.

3.2.2 *Influence of material variability on structural-acoustic response*

Two case studies are considered to show the influence of the material variability on the dynamic response in a structural-acoustic system as shown in Fig. 6. Fig. 6(a) shows an interior rectangular cavity surrounded by three rigid walls and a constrained-layer-damping beam with simply supported boundary condition. A unit force, F, is imposed on the center of the aluminum beam. Fig. 6(b) illustrates an air duct that consists of four flat panels under harmonic pressure loading. Four constrained-layer damping patches are bonded on the center of the panels to reduce the radiated sound power into infinite air space.

The four variables (a_0, a_1, c_1, β) in the fractional derivative model and operational temperature (or shift factor, α) are selected as the random variables as listed in Table 1. For the structure in Fig. 6(a), the sound pressure levels at a point A are calculated with one thousand random samples of the random variables generated by Monte Carlo simulation. For the structure in Fig. 6(b), the radiated powers are calculated with one thousand random samples. Figs. 7(a) and (b) show the calculated variability bound (with 95% confidence interval) of the sound pressure level in a decibel scale over a specified frequency range. The magnitude of the amplitude variation at the peak is beyond 10 dB. Because the variability of the viscoelastic damping material causes large variability on the acoustic responses of the structural-acoustic systems, it is important to

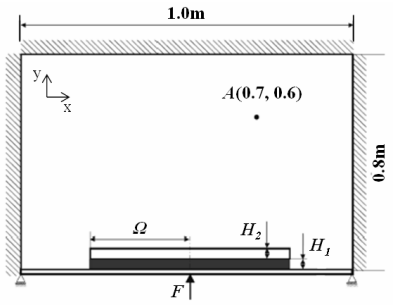

(a)

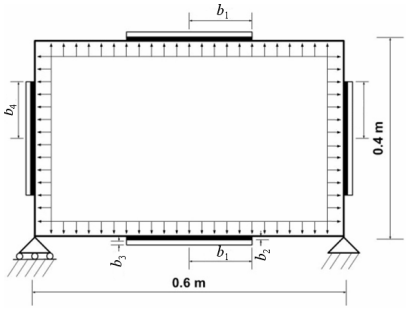

(b)

Fig. 6. Structural-acoustic systems with constrained-layer damping: (a) Rectangular cavity problem (for Case I, II); (b) Air duct radiation problem (for Case III and IV).

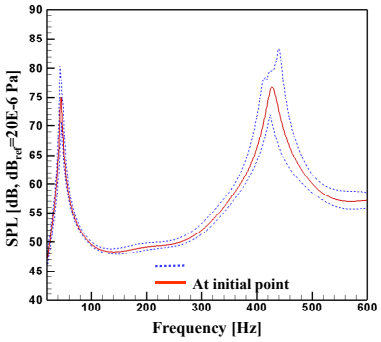

(a)

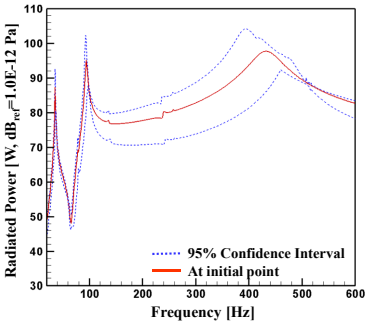

(b)

Fig. 7. Acoustic response variability in the structural-acoustic systems: (a) Rectangular cavity problem; (b) Air duct radiation problem.

Table 2. Design variables of the rectangular cavity problem.

Design variable	Initial value	Lower bound	Upper bound	COV	Distribution type
Ω [m]	0.2	0.1	0.45	1%	Normal
H_1 [mm]	0.5	0.1	3	10%	Normal
H_2 [mm]	5	1	10	5%	Normal

Table 3. Variance of the location for sound pressure calculation.

	Lower bound	Upper bound	Distribution type
A_x	0.6	0.8	Beta(2, 2)
A_y	0.5	0.7	Beta(2, 2)

consider the variability in the optimization of a damping layer design.

4. Reliability-based design optimization of the structural-acoustic systems

The design objective of a constrained-layer damping treatment in structural-acoustic systems is to maximize the robustness of acoustic responses while minimizing the amount of the damping layer and satisfying a reliability target on the acoustic response. Sections 4.1 and 4.2 deal with RBDO formulations and results for the problems in Fig. 6(a) and (b), respectively.

4.1 Reliability-based design optimization of the rectangular cavity problem

A simple rectangular cavity problem surrounded by a simply supported aluminum beam with a constrained-layer damping in Fig. 6(a) is first considered for demonstration purposes. The ISD-110 damping material is used for the damping layer of the structure. The rectangular cavity problem has three design variables: the length of the constrained-layer (Ω), the thicknesses of the damping layer (H_1) and the constraining layer (H_2). The thickness of the base beam is 20 mm and remains constant during the optimization. The random variables for the damping material in Table 1 are used in the RBDO formulation. The manufacturing variability of the design variables is also considered. As listed in Table 2, their coefficients of variations (COVs) are assumed to be 1%, 10%, and 5%, respectively. In addition, the variance of the location for sound pressure calculation (point A in Fig. 6(a)) is considered by treating the coordinates of the location as random variables. In this study, it is assumed that the x and y coordinates of point A are distributed with the beta distribution as listed in Table 3 to reflect the uncertainty of the observation point.

The RBDO problem can be formulated as:

$$\begin{aligned} &\text{Find} && \mathbf{b}=\{\Omega, H_1, H_2\} \text{ such that} \\ &\text{Minimize} && \mu_\Phi + s_\Phi \\ &\text{Subject to} && P(G(\mathbf{b},\mathbf{X})<0) > R^t \\ & && \mathbf{b}_L \le \mathbf{b} \le \mathbf{b}_U \ , \mathbf{X}_L \le \mathbf{X} \le \mathbf{X}_U \end{aligned} \tag{13}$$

where $\mathbf{b}$ is the design variable vector; $\mathbf{X}$ is the random variable vector; Φ is the objective function; $P(\bullet)$ indicates probability; G is the constraint function; and R^t is the target reliability. The RBDO formulation minimizes the mean and standard deviation of the objective function for system robustness. The objective function is the weight performance in the damping structure as

$$\Phi(\mathbf{b}) = 2 \cdot \Omega \cdot \left(w_1 \cdot H_1 + w_2 \cdot H_2 \right) \cdot \xi_1 \tag{14}$$

where w_1 and w_2 are the densities of damping and constraining layers, respectively. ξ_1 is the width of the beam structure. Two performances are defined to represent the constraint function as

$$\begin{aligned} \Pi_1(\mathbf{b},\mathbf{X}) &= \int_{f_1}^{f_2} \left\langle 20\log\left(\|\zeta\| / \zeta_{ref} \right) - \zeta_{dB0} \right\rangle df \\ \Pi_2(\mathbf{b},\mathbf{X}) &= \int_{f_1}^{f_2} \zeta^2 df \end{aligned} \tag{15}$$

where ζ is the sound pressure at point A, $\zeta_{ref} = 20.0\times10^{-6}$ Pa, ζ_{dB0} is a prescribed level in the decibel scale, and $\langle\zeta\rangle = \zeta$ if $\zeta > 0$, $\langle\zeta\rangle = 0$ otherwise. The first performance, $\Pi_1(\mathbf{b},\mathbf{X})$, is a sound pressure level, which corresponds to the integration of the sound pressure level beyond a target value (60 dB in Fig. 7) within a specified frequency range (e.g., up to 600 Hz in Fig. 7). The second performance, $\Pi_2(\mathbf{b},\mathbf{X})$, is an overall acoustic damping performance that corresponds to the sum of sound power within the frequency range. With these performances, the constraint functions can be defined as

$$G_i = \Pi_i - \Pi_{i0} \cdot G^t (i = 1,2) \quad \text{where} \quad G^t = 0.95 \tag{16}$$

where Π_{i0} is the functional value of Π_i at initial design, and G^t refers to the target constraint value. Two cases of the rectangular cavity design problem were conducted for each constraint function: Case I with G_1 and Case II with G_2.

The RBDO problems defined in Eqs. (13) to (16) are solved for the rectangular cavity (Fig. 6(a)) problem using the SQP algorithm in MATLAB (2007). Case I (or Case II) considers G_1 (or G_2) as the constraint function, respectively. The frequency responses (Π_1, Π_2) and the design sensitivity information are calculated using the discretized boundary element matrices and used for the optimization. The constrained-layer damping beam in the rectangular cavity is discretized with 20 elements: the 10-DOF finite elements for the constrained part, and the degenerated elements for the bare part. The acoustic cavity is discretized with 80 quadratic boundary elements. The EDR method uses 41 analysis calls ($4\times N+1$, N is the number of random variables in Table 1 to 3) for estimating the objective function and constraint in a probabilistic manner. The target reliability (R^t) is set to 3-sigma level (99.865%). For each case deterministic design optimization (DDO) is first performed and the results are compared with the RBDO results. RBDO uses the statistical information of the random

Table 4. The optimization results of Case I and Case II.

		Initial		DDO		RBDO	
		Case I	Case II	Case I	Case II	Case I	Case II
b	Ω [m]	0.20	0.20	0.1000	0.1163	0.1419	0.1430
	H1 [mm]	0.50	0.50	0.1838	0.2127	0.1781	0.1777
	H2 [mm]	5.00	5.00	7.0553	6.5335	9.7632	9.7611
Φ		0.286	0.2856	0.1965	0.2121	0.4042	0.4072
Reli-ability	EDR	18.7	19.25	45.34	56.03	99.865	99.865
	MCS	-	-	-	-	99.8	99.8

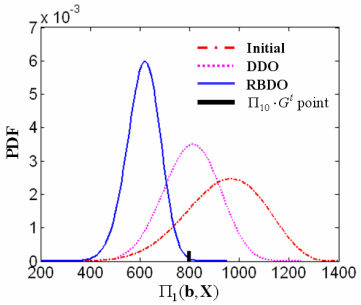

(a)

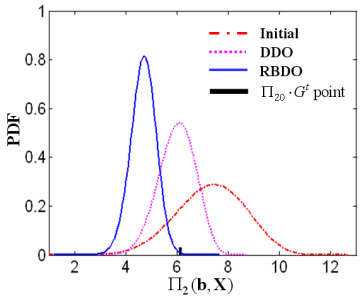

(b)

Fig. 8. PDFs of the constraint: initial, deterministic optimization and RBDO design points: (a) Case I; (b) Case II.

variables shown in Tables 1, 2 and 3. The optimization results of Case I and Case II are listed in Table 4.

When RBDO results are compared with the initial model, the weight performances (design objective) for Case I and II are sacrificed to improve the reliability of the acoustic performance (design requirement) to 3-sigma level by about 41.5% and 42.6%, respectively. In RBDO, the acoustic performances become reliable by reducing overall sound pressure level. As found in Table 4, the deterministic optimum designs turn out to be unreliable (45.34%, 56.03% reliability for Case I and II, respectively). The design becomes reliable by increasing the total amount of the damping material (the objective function). This underscores the strong need to consider the uncertainties in the design of constrained-layer damping layout.

Fig. 8 shows the PDFs of each constraint at the initial, deterministic, and reliability-based optimum design points. The acoustic performances (design requirement) are considerably

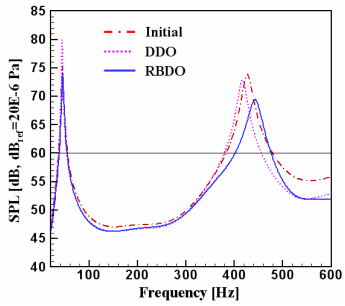

(a)

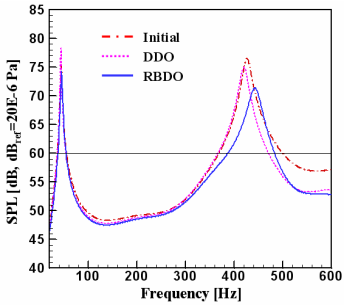

(b)

Fig. 9. Acoustic responses: initial, deterministic optimization and RBDO points: (a) Case I; (b) Case II.

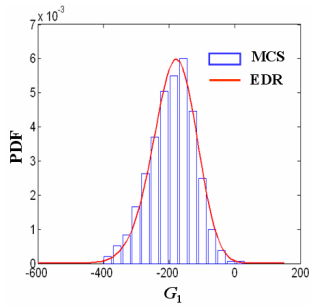

(a)

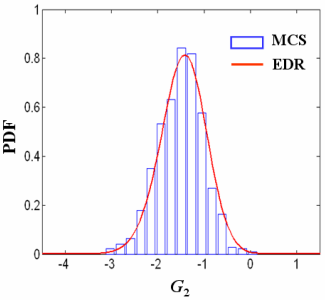

(b)

Fig. 10. MCS and EDR results: (a) Case I; (b) Case II.

improved to meet the reliability requirements. Fig. 9 shows the sound pressure responses at the three different design points. As the design is improved from the initial to RBDO, it is clearly shown that the design requirement (damping performance) becomes reliable by increasing the damping performance. In Fig. 10, the PDF of G_1 from the EDR method is

Table 5. Design variables of the air duct radiation problem.

Design Variable	Initial Value	Lower Bound	Upper Bound
b_1 [m]	0.15	0.1	0.29
b_2 [mm]	1.5	0.1	3
b_3 [mm]	5	1	10
b_4 [m]	0.15	0.1	0.19

compared with the histogram from MC simulation with 1,000 random samples at the RBDO optimal design. Results show that the EDR method very accurately predicts the PDF and reliability in structural-acoustic systems.

4.2 Reliability-based design optimization of the air duct radiation problem

The air duct radiation problem in Fig. 6(b) has four design variables as shown in Table 5: the length of the constraining layer in the top and bottom panels (b_1), the thicknesses of the damping layer (b_2), the thickness of the constraining layer (b_3), and the length of the constraining layer in the left and right panels (b_4). The thickness of the base beam is 2 mm and remains constant during the optimization. In this problem, the variability of ISD-110 damping material in Table 1 only is considered.

The RBDO problem is formulated as:

$$\begin{aligned} &\text{Find} && \mathbf{b}=\{b_1, b_2, b_3, b_4\} \text{ such that} \\ &\text{Minimize} && \mu_\Phi + s_\Phi \\ &\text{Subject to} && P(G(\mathbf{b},\mathbf{X})<0) > R^t \\ & && \mathbf{b}_{\mathrm{L}} \le \mathbf{b} \le \mathbf{b}_U \ , \ \mathbf{X}_{\mathrm{L}} \le \mathbf{X} \le \mathbf{X}_{\mathrm{U}} \end{aligned} \tag{17}$$

Here, the objective function is the weight of the damping structure as

$$\Phi(\mathbf{b}) = 4\cdot(b_1+b_4)\cdot\left(w_3\cdot b_2 + w_4\cdot b_3\right)\cdot\xi_2 \tag{18}$$

where w_3 and w_4 are the densities of damping and constraining layers, respectively. ξ_2 is the width of the beam structure. Two performance functions are defined to represent the constraint functions as

$$\begin{aligned} &\Pi_3(\mathbf{b},\mathbf{X}) = \int_{f_1}^{f_2} \left\langle 10\log\left(\|r\|/r_{ref}\right) - r_{dB0}\right\rangle df \\ &\Pi_4(\mathbf{b},\mathbf{X}) = \int_{f_1}^{f_2} r\, df \quad \left(r = \frac{1}{2}\int_\Gamma \mathrm{Re}[\zeta\overline{v}_n]d\Gamma\right) \end{aligned} \tag{19}$$

where r is radiated power from the structure into the air medium, v_{n} is outward-normal velocity of the structure to the boundary, and the overbar(-) represents complex conjugate of the argument. r_{ref} is 1.0×10^{-12} W, and r_{dB0} is a prescribed level in the decibel scale. The first function, $\Pi_3(\mathbf{b},\mathbf{X})$, is a radiated sound power performance, which corresponds to the integration of the radiated sound power graph beyond a target value (80 dB) within a specified frequency range (e.g., up to 600 Hz in Fig. 7). The second function, $\Pi_4(\mathbf{b},\mathbf{X})$, is the sum of radiated sound power performance within the frequency range. Then, the constraint functions can be defined as

$$G_i = \Pi_i - \Pi_{i0}\cdot G^t (i=3,4) \quad \text{where } G^t = 0.5 \tag{20}$$

where Π_{i0} is the functional value of Π_i at initial design, and G^t refers to the target constraint value. Two cases of the air duct radiation design problem were conducted for each constraint function: Case III with G_3 and Case IV with G_4.

Table 6. The optimization results of Case III and Case IV.

		Initial		DDO		RBDO	
		Case III	Case IV	Case III	Case IV	Case III	Case IV
b	b_1[m]	0.15	0.15	0.1519	0.1379	0.29	0.2780
	b_2 [mm]	1.5	1.5	2.6009	2.8587	3.0	3.0
	b_3 [mm]	5	5	1.0	1.0	1.9390	1.0
	b_4 [m]	0.15	0.15	0.1	0.1	0.1	0.1
Φ		1.6573	1.6573	0.4810	0.4758	1.1653	0.7601
Reliability	EDR	0.835	18.74	45.76	0.4179	99.865	99.865
	MCS	-	-	-	-	99.8	99.8

DDO and RBDO are performed by considering the variability in the ISD-110 damping material. The target reliability of this RBDO problem (R^t) in Eq. (17) is also set to 3-sigma level (99.865%). The optimization results of Case III and Case IV are listed in Table 6.

In the DDO results, b_3 and b_4 have converged at the low bounds. This result can be analyzed from the main effect plot in Fig. 11. This plot indicates the average response at each level of design variables. In this plot each design variable is set to have four levels. These plots show larger sensitivities of G_3 and G_4 with respect to b_1 and b_2 than those with respect to b_3 and b_4. Based on these plots, it is analyzed that b_3 and b_4 contribute to the minimization of the objective function rather than to the constraint satisfaction. Fig. 12 shows the PDFs of the constraint. As observed in the previous section, the RBDO results show the design with the reliability constraints satisfied: most of the PDF is located below $\Pi_{i0}\cdot G^t$ in Eq. (20) (the black bar in Fig. 12).

Table 6 shows that the acoustic performance (design requirement) becomes reliable by increasing the total amount of the damping material. That is, the weight performances (design objective) are sacrificed to improve the reliability of the acoustic performance to 3-sigma level (0.48 to 1.17 for Case III, 0.48 to 0.76 for Case IV).

Fig. 13 shows the acoustic responses at the initial, DDO, and RBDO design points. It is evident that the design requirement (radiated power) becomes reliable by increasing the amount of damping material.

Fig. 14 shows the mode shapes at the initial condition.

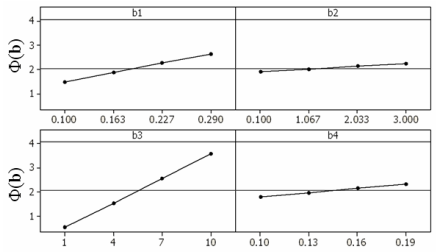

(a)

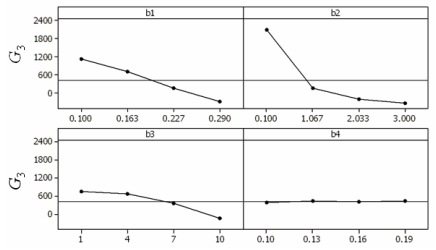

(b)

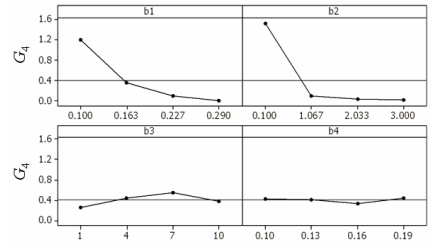

(c)

Fig. 11. Main effect plot for : (a) the object function; (b) the constraint function G_3; (c) the constraint function G_4.

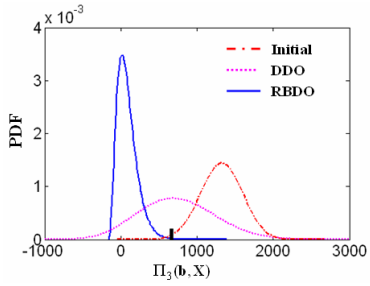

(a)

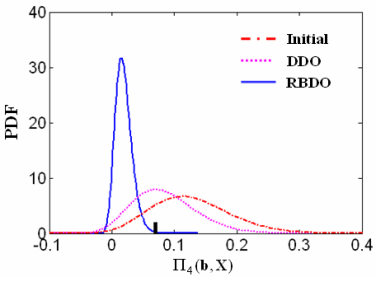

(b)

Fig. 12. PDFs of the constraint: initial, deterministic optimization and RBDO points: (a) Case III; (b) Case IV.

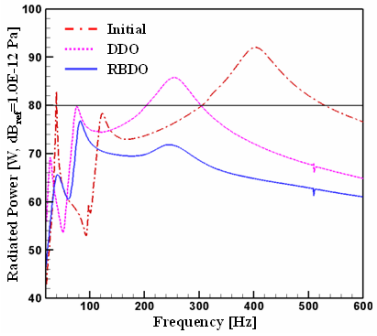

(a)

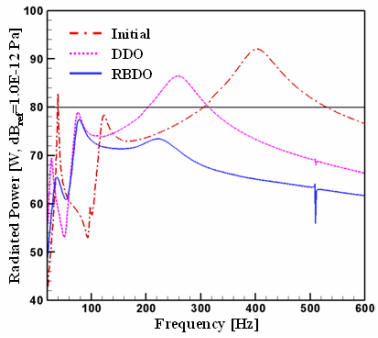

(b)

Fig. 13. Acoustic response: initial, deterministic optimization and RBDO points: (a) Case III; (b) Case IV.

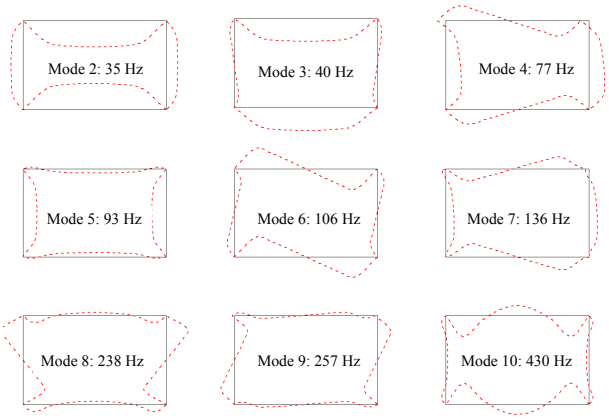

Fig. 14. Mode shapes of the air duct radiation problem.

Noting that the pressure loading in the air duct radiation problem is in-phase on the four panels, it can be seen that three modes (mode 2, mode 5 and mode 10) are excited by the loading in Fig. 14. In addition, from the mode shapes we can understand why the contribution of the side panels is less dominant in the constraint functions than that of the top and bottom panels: the acoustic response especially around 430 Hz (Mode 10) is reduced significantly where the relative vibration of the side panel is minimal.

5. Conclusion

This paper proposes a statistical modeling method using sta-

tistical calibration method for viscoelastic damping material and applies it to the reliability based design optimization of the constrained-layer damping layouts in structural-acoustic systems. In the modeling of the viscoelastic damping material, two factors on the variability in the complex modulus were considered: operational temperature variation and experimental/model errors. The statistical calibration method characterized the variability of the complex modulus by maximizing the agreement with all available experimental data (storage shear modulus and loss factor data) using the likelihood function metric. The statistical calibration method can be easily expanded to other viscoelastic constitutive models for the variability characterization of the damping material property.

Operational condition variability, in addition to the material property variability, was considered in the reliability-based robust designs of the constrained-layer damping layout. Two structural-acoustic systems were considered with acoustic performance requirements. It was demonstrated that the variability of the damping material is significantly propagated to that of the acoustic performances in two structural-acoustic systems. For the rectangular cavity problem, variability on manufacturing, the location for sound pressure calculation, the operational temperature, and the damping material were considered. The weights (design objective) were increased by about 40%, while the reliability of the acoustic performance (sound pressure and power) requirement was improved to 99.865%. This formulation can be applicable for the damping layout design in a passenger vehicle to achieve robust and reliable cabin noise reduction. As an example of a sound radiation problem, an air duct problem with constraint on a radiated sound power, was introduced and solved. This formulation can be applicable for general structure-borne noise problems in, for example, electronic appliances and automobiles. The numerical results show that RBDO yields more robust and reliable damping layout designs than the deterministic design optimization.

Acknowledgment

This work was supported by the U.S. National Science Foundation (NSF) under Grant No. GOALI-0729424, by the National Research Foundation of Korea (NRF) grant (No. R01-2007-000-10986-0), and by the SNU-IAMD.

References

[1] D. I. G. Jones, *Handbook of viscoelastic vibration damping*, Wiley, New York, USA (2001).

[2] A. Baz, J. Ro, Optimum design and control of active constrained layer damping, *ASME J. Mech. Design*, 117 (1995) 135-144.

[3] T. W. Kim and J. H. Kim, Eigensensitivity based optimal distribution of a viscoelastic damping layer for a flexible beam, *J. Sound Vib.*, 273 (2004) 201-218.

[4] D. H. Lee, Optimal placement of a constrained-layer damping for reduction of interior noise, *AIAA J.*, 46 (2008) 75-83.

[5] D. H. Lee and W. S. Hwang, Layout optimization of an unconstrained viscoelastic layer on beams using fractional derivative model, *AIAA J.*, 42 (2004) 2167-2170.

[6] B. C. Nakra, Vibration control in machines and structures using viscoelastic damping, *J. Sound Vib.*, 211 (1998) 449-465.

[7] S. Poh S, A. Baz A and B. Balachandran, Experimental adaptive control of sound radiation from a panel into an acoustic cavity using active constrained layer damping, *Smart Mater. Struct.*, 5 (1996) 649-659.

[8] H. Zheng and C. Cai, Minimization of sound radiation from baffled beams through optimization of partial constrained layer damping treatment, *Appl. Acoust.*, 65 (2004) 501-520.

[9] H. Zheng H, C. Cai C and X. M. Tan, Optimization of partial constrained layer damping treatment for vibrational energy minimization of vibrating beams, *Comput. Struct.*, 82 (2004) 2493-2570.

[10] B. C. Jung, D. H. Lee and B. D. Youn, Optimal design of constrained-layer damping considering material and operational condition variability, *AIAA J.*, 47 (2009) 2985-2995.

[11] K. Campbell, Statistical calibration of computer simulations, *Reliab. Eng. Syst. Safe*, 91 (2006) 1358-1363.

[12] D. J. McTavish and P. C. Hughes, Modeling of linear viscoelastic space structures, *J. Vib. Acoust.*, 115 (1993) 103-110.

[13] A. Calvi, Uncertainty-based loads analysis for spacecraft: Finite element model validation and dynamic responses, *Comput. Struct.*, 83 (2005) 1103-1112.

[14] D. W. Apley, J. Liu and W. Chen, Understanding the effects of model uncertainty in robust design with computer experiments, *ASME J. Mech. Design*, 128 (2006) 945-958.

[15] M. J. Bayarri, J. O. Berger, R. Paulo, J. Sacks, J. A. Cafeo, J. Cavendish, C. Lin and J. Tu, A framework for validation of computer models, *Technometrics*, 49 (2007) 138-154.

[16] D. Higdon, M. Kennedy, J. Cavendish, J. Cafeo, R. D. Ryne, Combining field data and computer simulations for calibration and prediction, *SIAM J Sci. Comput.*, 26 (2004) 448-466.

[17] M. C. Kennedy and A. O'Hagan, Bayesian calibration of computer models, *J. Royal Stat. Soc. Ser. B* (2001) 425-464.

[18] B. D. Youn and P. Wang, Bayesian reliability-based design optimization using eigenvector dimension reduction (EDR) method, *Struct. Multidis. Opt.*, 37 (2008) 1615-147.

[19] Y. Xiong, W. Chen, K. Tsui and D. Apley, A better understanding of model updating strategies in validating engineering models, *Comput. Meth. Appl. Mech. Eng.*,198 (2009) 1327-1337.

[20] B. D. Youn, Z. Xi and P. Wang, The Eigenvector dimension-reduction (EDR) method for sensitivity-free probability analysis, *Struct. Multidis. Opt.*, 37 (2008) 1615-1488.

[21] L. B. Eldred, W. P. Baker and A. N. Palazotto, Kelvin-voigt vs. fractional derivative model as constitutive relations for viscoelastic material, *AIAA J.*, 33 (1995) 547-550.

[22] S. Rahman S and H. Xu, A univariate dimension-reduction

method for multi-dimensional integration in stochastic mechanics, *Probabil. Eng. Mech.*, 19 (2004) 393-408.
[23] The MathWorksTM Inc. (2007) Matlab Software Package.

Byung C. Jung received his B.S. and M.S. in Mechanical Engineering from Hanyang University and KAIST, Korea, in 2002 and 2004, respectively. He is currently pursuing his Ph.D. in Mechanical Engineering from University of Maryland at College Park. His research interests include statistical model validation, RBDO, and energy harvester design. He was awarded a highlight of collections by smart materials and structures in 2009, and won the best paper prize in the division of Dynamics and Control by the Korean Society of Mechanical Engineering (KSME) in 2010.

Dooho Lee received the B.S. degree from Seoul National University, Korea in 1988, M.S. from KAIST, Korea in 1990, and the Ph.D. from KAIST, Korea in 1994. He worked for Samsung Motors, Inc. (1995-99), and is currently an associate professor in Dongeui University. His research focuses on design optimization of structural-acoustic systems, uncertainty propagation in dynamic problems, and sound transfer characteristics in human hearing system.

Byeng D. Youn received his Ph.D. from the Department of Mechanical Engineering in the University of Iowa, USA, in 2001. He was an Assistant Professor in Michigan Technical University (-2007), in the University of Maryland College Park (-2010), and currently in the School of Mechanical and Aerospace Engineering in Seoul National University, Republic of Korea. His research expertise includes: (1) reliability-based design, (2) prognostics and health management (PHM), and (3) energy harvester design. His dedicated effort has led to several notable awards, including the ISSMO/ Springer Prize in 2005 and over one hundred publications.

Soobum Lee received his Ph.D. in Mechanical Engineering from Korea Advanced Institute of Science and Technology (KAIST), Korea, in 2007. Currently he is a postdoctoral research associate at the department of Aerospace and Mechanical Engineering in the University of Notre Dame, USA. His main research interests include energy harvester design, topology optimization, robust design, and reliability based design optimization. He won the best paper prize in the division of CAE and computational mechanics by the Korean Society of Mechanical Engineering (KSME) in 2007, and was awarded a highlight of collections by smart materials and structures in 2009.